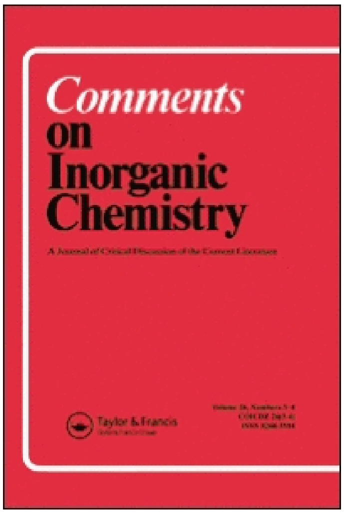

Comments on Inorganic Chemistry
Publication details, including instructions for authors and subscription information:
http://www.informaworld.com/smpp/title~content=t713455155

Direct and Superexchange Mechanisms for Optical and Thermal Electron Transfer and the Detectability of the Transition State by Radiative Spectral Emission

Aleksandr M. Kuznetsov[a]; Jens Ulstrup[b]
[a] The A. N. Frumkin Institute of Electrochemistry of the Academy of Sciences of the USSR, Moscow, USSR [b] Chemistry Department A, Building 207, The Technical University of Denmark, Lyngby, Denmark

To cite this Article Kuznetsov, Aleksandr M. and Ulstrup, Jens(1990) 'Direct and Superexchange Mechanisms for Optical and Thermal Electron Transfer and the Detectability of the Transition State by Radiative Spectral Emission', Comments on Inorganic Chemistry, 10: 4, 197 — 226

To link to this Article: DOI: 10.1080/02603599008048651

URL: http://dx.doi.org/10.1080/02603599008048651

Direct and Superexchange Mechanisms for Optical and Thermal Electron Transfer and the Detectability of the Transition State by Radiative Spectral Emission

ALEKSANDR M. KUZNETSOV
The A. N. Frumkin Institute of Electrochemistry of the
Academy of Sciences of the USSR,
Leninskij Prospect 31,
Moscow V-71, USSR

JENS ULSTRUP
Chemistry Department A,
Building 207,
The Technical University of Denmark,
2800 Lyngby, Denmark

We have reviewed a number of correlations between kinetic parameters which characterize optical and thermal electron transfer between two molecular sites. The correlations involve directly observables such as the molar absorptivity and emitted spectral distribution for optical and the rate constants for the thermal processes. We have also discussed the possible direct optical detection of the transition state configuration. This is feasible in principle by emission or Raman scattering from the first excited state in the adiabatic limit. The correlations can be extended both to optical and thermal electron transfer between metal or semiconductor electrodes and depolarizer molecules or molecular adsorbates, and to electron transfer in three-level, superexchange systems. In the latter case relations between superexchange rate constants and Raman scattering profiles can be pointed out.

Key Words: *intervalence transitions, superexchange, transition state, Raman scattering*

Comments Inorg. Chem.
1990, Vol. 10, Nos. 4 & 5, pp. 197–226
Reprints available directly from the publisher
Photocopying permitted by license only

1. INTRODUCTION

Transitions between two bound molecular or solid state Born–Oppenheimer electronic states can occur either by absorption or emission of light, or nonradiatively. In both cases the two states are coupled by an external perturbation and it has been recognized since the earliest theoretical approaches to electronic processes in molecules and solid state impurities that close formal relations between the two kinds of processes must therefore exist.[1,2] The quantitative form of such correlations must incorporate the transition probabilities of the processes, but in practical terms this must be extended to the appropriate observables. These are the rate constants for the thermal process, and either the molar absorptivity, the luminescence rate constant, the emission spectral distribution, or the excited state radiative lifetime for the optical process.

The correlations between optical and thermal processes acquired major new perspectives by extension to intervalence transitions in mixed-valence systems, reviewed and first classified by Allen and Hush[3,4] and by Robin and Day.[5] Weak near-infrared molecular intervalence transitions correspond to photo-induced electron transfer (ET) between the two sites and therefore represent a particularly close conceptual relation both to intramolecular thermal ET and to ET between mobile molecules in solution.[6,7] The corresponding band intensity and shape in this way becomes a sensitive probe for solvent and distance effects on the electronic-vibrational coupling in both kinds of processes.

Optical intervalence transitions often follow the behavior expected from ET theory combined with specific models for the solute-solvent systems.[6] Photo-induced ET would therefore in principle be an extremely powerful technique for the more elusive elements of ET theory such as the electronic exchange coupling and the inverted free energy range. Direct experimental documentation for both optical and thermal ET in a given binuclear system is, however, restricted to very few systems,[8-12] including a recent report on electron exchange in the $[\mathrm{Fe(CN)_6}]^{3-/4-}$ system in concentrated solutions.[13] This is due to the high thermal rate constants of the optically well characterized mixed-valence compounds and to the need for large concentrations of the "collision complex" which primarily contribute to optical intermolecular absorption in well-characterized thermal ET systems. In addition, well-characterized mixed-valence complexes always involve molecular bridge groups. These endow the transition with superexchange character which both increases the electronic coupling towards the adiabatic limit and gives a different structure to the electronic coupling compared with direct ET.

In this work we address in particular two aspects of the correlations between optical and thermal processes. The first concerns the nuclear configurations where the electronic transition occurs. Optical absorption and relaxed fluorescence proceeds primarily from the equilibrium nuclear configuration in the ground and excited state, respectively (Fig. 1), while the thermal process takes place at the saddle point region of the two potential surfaces. A central question is therefore the possible direct detection of the configuration at the saddle point by optical means, rather than indirectly via a rate constant or optical bandshape analysis. Such detection is obviously fraught with great technical difficulties caused by the strong vibrational excitation needed to reach the crossing

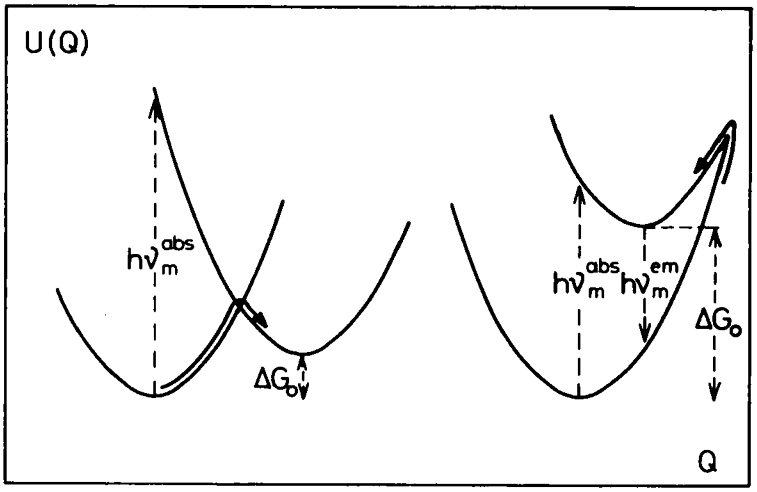

FIGURE 1 Different locations of initial and final state potential surfaces showing radiative absorption and emission (dashed arrows) and thermal transitions (fully drawn arrows).

and the corresponding low concentrations of these transition state complexes. However, as noted by Bersuker,[14] optical detection is also associated with a principal quantum mechanical problem, as detection requires that the state which interacts with the electromagnetic field is stationary.[15] This condition is only valid for potential wells whose depth approaches the kinetic energy of the system and applies only "inside" the reactants' and products' potential wells. On the other hand, the first excited state corresponding to two-site electronic transitions always has a pronounced potential minimum at the crossing. Detection of this region is therefore in principle feasible in the adiabatic limit by excited state emission, rather than ground state absorption.

The second point to be discussed is the extension of known correlations between "direct" optical and thermal ET to bridge group systems where the role of the bridge orbitals is explicitly specified. Such extension is possible by introducing bridge group or superexchange ET formalism and leads to interesting correlations between thermal superexchange ET rate constants and both single-photon absorption and Raman scattering probabilities.

We first provide a brief summary of some elements of ET theory and correlations between optical and thermal ET in direct transitions, based on observable quantities. Then we proceed to a discussion of the observability of the transition region, and we conclude by extensions of the correlations to electrochemical processes and to three-level processes as in superexchange ET and Raman scattering.

2. ELEMENTS OF DIABATIC ET THEORY AND CORRELATIONS BETWEEN THERMAL ET RATE CONSTANTS AND OBSERVABLES IN SINGLE-PHOTON ABSORPTION AND EMISSION PROCESSES

2.1. Correlations Between Thermal Rate Constants and Optical Single-Photon Observables

The most general form of the diabatic first order transition probability between the two electronic states "i" and "f" is, in the

Born–Oppenheimer and Condon approximations,[16–18]

$$W_{fi}^{\mathrm{th}}(\Delta G_0) = \frac{\beta}{i\hbar}\,(V_{fi}\,(\mathbf{Q}_{\mathrm{th}}^{*}))^2 e^{\beta G_i} \times \int_{-i\infty}^{i\infty} d\theta\ \mathrm{Tr}[\rho_i(1-\theta)\rho_f(\theta)]\ \exp(-\beta\theta\Delta G_0) \qquad (2.1)$$

where $\rho_i(1 - \theta)$ and $\rho_f(\theta)$ are the vibrational density matrices of the states "i" and "f" at the temperatures $T(1 - \theta)$ and T/θ, respectively, where T is the real temperature. ΔG_0 is the free energy gap (Fig. 1), $\beta = (k_B T)^{-1}$, where k_B is Boltzmann's constant, $\hbar$ is Planck's constant divided by 2π, $V_{fi}(Q_{\mathrm{th}}^{*})$ is the nondiagonal electron exchange matrix element at the saddle point of the potential surface crossing, $\mathbf{Q}_{\mathrm{th}}^{*}$, and the integration with respect to θ is along a contour parallel to the imaginary axis ($|\mathrm{Re}\theta| < 1$). G_i is finally the total vibrational energy in the state "i". Equation (2.1) can be converted to more specific forms by introducing explicit representations of the vibrational density matrices, to some of which we shall return below. The transition probability for optical single-photon absorption or spontaneous emission corresponding to the same two states, W_{fi}^{opt}, requires that the photon field characteristics are specified. By taking these as those of a narrow photon beam of random polarization we can give W_{fi}^{opt} the following form analogous to Eq. (2.1)[19,20]:

$$W_{fi}^{\mathrm{opt}}(\nu) = \frac{\beta}{i\hbar}(M_{fi}(\mathbf{Q}_{\mathrm{opt}}^{*}))^2 e^{\beta G_i} \times \int_{-i\infty}^{i\infty} d\theta\ \mathrm{Tr}[\rho_i(1-\theta)\rho_f(\theta)]\ \exp[-\beta\theta(\Delta G_0 \pm h\nu)] \qquad (2.2)$$

where ν is the frequency of the absorbed or emitted light, corresponding to the "minus" and "plus" sign, respectively, and $M_{fi}(\mathbf{Q}_{\mathrm{opt}}^{*})$ is the transition dipole matrix element at the nuclear configuration $\mathbf{Q}_{\mathrm{opt}}^{*}$. In general $\mathbf{Q}_{\mathrm{opt}}^{*}$ is close to the equilibrium configuration of the ground and excited state for absorption and emission, respectively. The difference between $\mathbf{Q}_{\mathrm{opt}}^{*}$ and $\mathbf{Q}_{\mathrm{th}}^{*}$ is important for intersite electronic transitions where the electronic wave functions are exposed to environmental nuclear configurational fluctuations.[21–23]

Equations (2.1) and (2.2) provide a simple general correlation between the transition probabilities for the two kinds of processes. Such correlations are, however, more useful if they apply to the observables of the processes. This is so much the more important as Eq. (2.2), although formally analogous to Eq. (2.1), is not directly comparable to the latter since W_{fi}^{th} is a rate constant while W_{fi}^{opt} contains an additional energy density. The optical absorption process is suitably characterized by the molar absorptivity, $\kappa_{fi}(\nu)$ while emission is characterized either by the emitted spectral density distribution in all directions, $I_{\mathrm{sp,em}}(\nu)$, or by the radiative lifetime τ_r. The relation between $W_{fi}^{\mathrm{opt}}(\nu)$ and $\kappa_{fi}(\nu)$ is thus[20]

$$\kappa_{fi}(\nu) = \frac{2\pi}{3c}\, h\nu\; W_{fi}^{\mathrm{opt}}(\nu) \tag{2.3}$$

where c is the light velocity in the medium and accounts for the environmental modulation of the incoming electromagnetic field. The relations between W_{fi}^{opt} and $I_{\mathrm{sp,em}}(\nu)$ or τ_r are, respectively,

$$I_{\mathrm{sp,em}}(\nu) = \frac{4}{\pi c^3}\, \nu^4\, \Delta\nu \hbar^2 W_{fi}^{\mathrm{opt}}(\nu), \tag{2.4}$$

$$\tau_r^{-1} = \frac{4}{\pi c^3} \int_0^\infty h\nu^3 W_{fi}^{\mathrm{opt}}\, (\nu) d\nu \tag{2.5}$$

where $\Delta\nu$ is to be viewed as an instrument property.

Combination of Eqs. (2.1)–(2.5) provides the following correlations between the observables for the thermal and optical processes

$$\kappa_{fi}(\nu) = \frac{2\pi}{3c} h\nu [M_{fi}(\mathrm{Q}_{\mathrm{opt}}^*)/V(\mathrm{Q}_{\mathrm{th}}^*)]^2\, W_{fi}^{\mathrm{th}}(\Delta G_0 - h\nu), \tag{2.6}$$

$$I_{\mathrm{sp,em}}(\nu) = \frac{4}{\pi c^3}(h\nu)^2\nu^2\Delta\nu[M_{fi}(\mathrm{Q}_{\mathrm{opt}}^*)/V_{fi}(\mathrm{Q}_{\mathrm{th}}^*)]^2\, W_{fi}^{\mathrm{th}}(\Delta G_0 + h\nu), \tag{2.7}$$

$$\tau_r^{-1} = \frac{4}{\pi c^3}\int_0^\infty (h\nu)\nu^2[M_{fi}(\mathrm{Q}_{\mathrm{opt}}^*)/V_{fi}(\mathrm{Q}_{\mathrm{th}}^*)]^2\, W_{fi}^{\mathrm{th}}(\Delta G_0 + h\nu)d\nu, \tag{2.8}$$

where the combination of electronic factors may in principle also depend on ν when substantial charge displacements exposed to solvent configurational fluctuations accompany the process.[21-23]

2.2. Specific Bandshape Expressions for Diabatic Electronic Transitions in Vibrationally Dispersive Media

As a frame of reference we introduce a specific but broadly representative model for the solute–solvent system. The intramolecular and solvent coordinates are regarded as separate normal mode sets, the former represented by a set of displaced harmonic oscillators, the latter as a linear, frequency dispersive medium,[19,24,25] the dispersion being in principle essential to ensure convergent rate expressions.[26] $W_{fi}^{\mathrm{th}}(\Delta G_0)$ then takes the form

$$W_{fi}^{\mathrm{th}}(\Delta G_0) = \frac{\beta}{i\hbar}(V_{fi})^2 \int_{-i\infty}^{i\infty} d\theta \exp[-\beta\theta\Delta G_0 - F_m(\theta)]\,Tr[\exp(\beta F_i^{(c)})\rho_i^{(c)}(1-\theta)\rho_f^{(c)}(\theta)] \tag{2.9}$$

where the superscript "(c)" refers to the molecular modes only. The solvent function $F_m(\theta)$ has the form

$$F_m(\theta) = \frac{1}{\hbar}\int_0^\infty d\omega\,\mathscr{E}_s(\omega)\,\frac{sh[(1/2)\beta\hbar\omega(1-\theta)]\,sh((1/2)\beta\hbar\omega\theta)}{sh((1/2)\beta\hbar\omega)}, \tag{2.10}$$

where $\mathscr{E}_s(\omega)$ is the solvent reorganization free energy density. In its most general quantum mechanical form, $\mathscr{E}_s(\omega)$ is given by the Fourier transform of the retarded Green's function of the inertial polarization fluctuations, i.e.,[24-27]

$$\mathscr{E}_s(\omega) = \frac{2}{\pi}\int d\mathbf{r}\,d\mathbf{r}'\Delta E_\alpha(\mathbf{r})\,\Delta E_\beta(\mathbf{r}')\,\frac{1}{\omega}\,\mathrm{Im}G^R(\mathbf{r},\mathbf{r}';\,\omega), \tag{2.11}$$

where α and β $(= x,y,z)$ are space coordinates, $\mathbf{r}$ and $\mathbf{r}'$ are space vectors and $\Delta\mathbf{E}(\mathbf{r})$ is the difference between the vacuum fields of the molecular charge distribution in the initial and final states.

The Green's function is specifically the quantum statistical average of the inertial polarization components $P_{\alpha,\beta}(\mathbf{r},t)$,[27]

$$G^R_{\alpha\beta}(\mathbf{r},\mathbf{r}';\, t,t') = -\frac{i}{\hbar}\,\theta(t - t')\langle[P_\alpha(\mathbf{r},t)P_\beta(\mathbf{r}',t')]\rangle, \tag{2.12}$$

$\theta(t - t')$ being the step function. For practical use of Eq. (2.11) the field terms and $G^R_{\alpha\beta}(\mathbf{r},\mathbf{r}';\, \omega)$ are, however, more conveniently brought to rest on specific electrostatic models and models for the solvent frequency dispersion, respectively. For example, if the solvent is homogeneous and isotropic, then[24–26]

$$\begin{gathered}\mathrm{Im}G^R(\omega) = \frac{1}{4\pi}\frac{\mathrm{Im}\varepsilon(\omega)}{|\varepsilon(\omega)|^2}; \quad \mathscr{E}_s(\omega) = \frac{2E_s}{\pi\omega c}\frac{\mathrm{Im}\varepsilon(\omega)}{|\varepsilon(\omega)|^2};\\ c = \varepsilon_0^{-1} - \varepsilon_s^{-1}; \quad E_s = \int_0^\infty d\omega\mathscr{E}_s(\omega),\end{gathered} \tag{2.13}$$

where $\varepsilon(\omega)$ is the dielectric permittivity function, ε_0 is the optical and ε_s the static dielectric constant, while E_s is the total solvent reorganization free energy.

$\mathrm{Im}G^R(\omega)$ or $\varepsilon(\omega)$ contains all information of the real solvent vibrational spectrum. For water this is well represented by a combination of Debye and resonance bands[28]:

$$\varepsilon_D(\omega) = \varepsilon_0 + \frac{\varepsilon_s - \varepsilon_0}{1 - i\omega\tau_D}, \tag{2.14}$$

$$\varepsilon_R(\omega) = \varepsilon_0 + \tfrac{1}{2}(\varepsilon_s - \varepsilon_0)\left[\frac{1 - i\omega_R\Gamma_R}{1 - i(\omega + \omega_R)\Gamma_R} + \frac{1 + i\omega_R\Gamma_R}{1 - i(\omega - \omega_R)\Gamma_R}\right], \tag{2.15}$$

τ_D^{-1} being the Debye and ω_R the resonance frequency, and Γ_R is the damping coefficient.

Further conversion to specific bandshape forms are conveniently referred to the crucial limits of weak and strong solute–solvent coupling. For broad bands these are determined by the conditions[19]

$$(E_s/\hbar\omega_m)\mathrm{cth}\ ((1/2)\beta\hbar\omega_m) > 1 \text{ and } < 1, \tag{2.16}$$

respectively, where ω_m is the maximum of the resonance. The "coupling strength" thus depends on T, the low- and high-T limits being $E_s/\hbar\omega_m$ and $2E_s/\beta(\hbar\omega_m)^2$, respectively. The strong-coupling limit is what prevails for all real thermal and optical ET processes, but for the sake of completion we provide both limiting bandshape forms. We consider first coupling solely to the medium.

2.2.1. *The Weak-Coupling Limit*

The following bandshape form emerges at all T^{25}:

$$W_{fi}^{\text{th}}(\Delta G_0) = \frac{2\pi}{\hbar}\frac{1}{\gamma}(V_{fi})^2 \frac{\gamma^2}{(\Delta G_0)^2 + \gamma^2};$$
$$\gamma = \frac{1}{\hbar\omega_m} k_B T E_s << 1. \tag{2.17}$$

In the weak-coupling limit the solute–solvent interaction thus gives a Lorentzian band which does not depend on the detailed solvent spectral features. The bandwidth, γ, is determined by the temperature and the coupling strength and vanishes as $T \to 0$. The maximum for the corresponding optical transition, $h\nu_m$, is at

$$h\nu_m \approx \Delta G_0, \tag{2.18}$$

giving also, for a narrow band, the form

$$W_{fi}^{\text{th}}(\Delta G_0) \approx W_{fi}^{\text{th}}(h\nu_m) \approx \frac{2\pi}{\hbar}(V_{fi})^2 \frac{\gamma}{(h\nu_m)^2}. \tag{2.19}$$

2.2.2. *The Strong-Coupling Limit*

In this limit the bandshape is more sensitive to the details of the solvent spectrum. This is illustrated if we invoke the simplifying assumption that the whole spectrum can be divided into a low-frequency, classical group of bands and a group of high-frequency bands, with a small density of states in the frequency range $k_BT/\hbar$. We then obtain, close to the maximum of the optical process or to the activationless free energy range of the thermal process,[19,20,25]

$$W_{fi}^{\text{th}}(\Delta G_0) = \frac{2\sqrt{\pi}}{\hbar\Delta_s}(V_{fi})^2 \exp\left[-\frac{(E_s + \Delta G_0)^2}{\Delta_s^2}\right],$$

$$\Delta_s = 2\left[\frac{\hbar E_s}{\pi c}\int_0^\infty d\omega \frac{\text{Im}\varepsilon(\omega)}{|\varepsilon(\omega)|^2}\text{cth}((1/2)\beta\hbar\omega)\right]^{1/2} \equiv \Delta_s^{cl} + \Delta_s^{qu}, \qquad (2.20)$$

$$\Delta_s^{cl} \approx 2\sqrt{k_B T E_s^{cl}}; \quad \Delta_s^{qu} \approx \sqrt{2\hbar\omega_{qu}E_s^{qu}},$$

where E_s^{cl} and E_s^{qu} refer to the low- and high-frequency parts of the spectrum, respectively, and ω_{qu} is the center of the high-frequency distribution. More specifically

$$E_s^{cl} = \frac{2E_s}{\pi c}\int_0^{k_BT/\hbar} \frac{d\omega}{\omega}\frac{\text{Im}\varepsilon(\omega)}{|\varepsilon(\omega)|^2}; \qquad (2.21)$$

$$E_s^{qu} = \frac{2E_s}{\pi c}\int_{k_BT/\hbar}^{\infty} \frac{d\omega}{\omega}\frac{\text{Im}\varepsilon(\omega)}{|\varepsilon(\omega)|^2}, \qquad (2.22)$$

$$\omega_{qu}E_s^{qu} = \frac{2E_s}{\pi c}\int_{k_BT/\hbar}^{\infty} d\omega \frac{\text{Im}\varepsilon(\omega)}{|\varepsilon(\omega)|^2}.$$

Moreover, for the optical process,

$$h\nu_m = \Delta G_0 + E_s^{cl} + E_s^{qu}. \qquad (2.23)$$

As shown elsewhere,[19] the Gaussian form in Eq. (2.20) is only valid close to the maximum, cubic and higher terms in the exponent being important in the band wings. In the normal free energy range ($|\Delta G_0| << E_s$),

$$W_{fi}^{\text{th}}(\Delta G_0) = \frac{2\sqrt{\pi}}{\hbar\Delta_s^{cl}}(V_{fi})^2 \exp\left(-\frac{E_s^{qu}}{\hbar\omega_{qu}}\right)$$
$$\times \exp\left[-\frac{(E_s^{cl} + \Delta G_0)^2}{(\Delta_s^{cl})^2}\right]. \qquad (2.24)$$

Equations (2.20)–(2.24) give the following correlation between the activation (free) energy for the thermal process, E_A, and the maximum for radiative absorption

$$E_A = (h\nu_m - E_s^{qu})^2/4(h\nu_m - \Delta G_0 - E_s^{qu}). \qquad (2.25)$$

The corresponding equation for the fully classical solvent behavior ($E_s^{qu} = 0$), first obtained by Hush,[4] is

$$E_A^{cl} = (h\nu_m)^2/4(h\nu_m - \Delta G_0). \qquad (2.26)$$

Vibrational dispersion thus gives a different correlation which in principle could serve as a basis for determination of the high-frequency contribution to E_s.

2.3. Intramolecular Mode Reorganization and Bandwidth Temperature Dependence

The effects of intramolecular reorganization on the optical bandshape features and thermal free energy relations have been discussed in detail elsewhere.[7,16–20,29,30] This extends to a variety of representations of these modes including mode displacement and distortion, anharmonicity, and normal mode mixing. Presently we invoke only a single element of importance directly to the correlations between optical and thermal two-level processes. This relates to the temperature dependence of the Gaussian bandwidth and constitutes an additional consistency check of Eqs. (2.24)–(2.26).

In the presence of displaced harmonic modes all equations in Section 2.2 maintain full validity except that E_s^{cl} is everywhere replaced by the total classical reorganization free energy in both the solvent and the low-frequency molecular modes, E_r^{cl}, and E_s^{qu} similarly by the high-frequency reorganization free energy in both mode sets, E_r^{qu}. E_r^{cl} and E_r^{qu} can then be separated in a twofold fashion, namely either by Eq. (2.26) or by the temperature dependence of the Gaussian bandwidth, since the square of the latter depends linearly on T and the extrapolated value at $T \rightarrow 0$ is $2\hbar\omega_{qu}E_r^{qu}$. This separation is sharp for vanishing E_s^{qu} but somewhat blurred for finite values of the high-frequency solvent contribution due to the large widths of the solvent absorption bands.

2.4. Cross Correlations

One of the most widely used frames for correlating thermal electron transfer data is the Marcus cross relation[31,32]

$$k_{12} = \sqrt{k_{11}k_{22}k_{12}f}; \quad \ln f = (\ln K_{12})^2/4\ \ln(k_{11}k_{22}/Z^2), \qquad (2.27)$$

where k_{11} and k_{22} are the rate constants of the two exchange reactions, while k_{12} is the rate constant and K_{12} the equilibrium constant for the cross reaction. Z is the total pre-exponential factor in the high-temperature rate constant. Equation (2.27) rests on a range of assumptions including: (a) high-temperature and harmonic behavior of all nuclear modes; (b) adiabatic limits of the rate constants; (c) cancellation of intermolecular work terms, and (d) the total reorganization free energy of the cross reaction being the arithmetic average of those for the exchange reactions.

Correlations between rate parameters of thermal and optical processes offers an extension of cross relations to the latter and a way of relaxing most of the conditions on which Eq. (2.27) rests. Provided that only the high-frequency part of the combined solvent and molecular modes satisfies the cross condition $E^{qu}_{r(12)} = \frac{1}{2}(E^{qu}_{r(11)} + E^{qu}_{r(22)})$ where the subscripts refer to the different reactions, then the following correlation between the rate parameters of the optical and thermal processes is valid:

$$E_A^{(12)} = [h\nu_m^{(12)} - \tfrac{1}{2}(h\nu_m^{(11)} - 4E_A^{(11)}) - \tfrac{1}{2}(h\nu_m^{(22)} - 4E_A^{(22)})]^2$$

$$\times \{4[h\nu_m^{(12)} - \tfrac{1}{2}(h\nu_m^{(11)} - 4E_A^{(11)}) - \tfrac{1}{2}(h\nu_m^{(22)} - 4E_A^{(22)}) - \Delta G_0^{(12)}]\}^{-1}. \qquad (2.28)$$

This form rests on no conditions regarding the classical reorganization free energy and the electronic factor. If the assumption that $E^{cl}_{r(12)} = (1/2)(E^{cl}_{r(11)} + E^{cl}_{r(22)})$ is also invoked, then Eq. (2.28) takes the simpler form

$$h\nu_m^{(12)} = \tfrac{1}{2}(h\nu_m^{(11)} + h\nu_m^{(22)}) + \Delta G_0^{(12)}. \qquad (2.29)$$

3. THE ADIABATIC LIMIT OF ELECTRON TRANSFER

Most of the considerations in Section 2 refer to the diabatic limit of small splittings at the crossing of the two potential surfaces. In this section we consider briefly the opposite, adiabatic limit which is particularly important in possible attempts to detect this region.

The adiabatic limit prevails when the electron exchange integral is large, i.e., when the following inequalities are valid for low- and high-frequency modes, respectively:

$$(V_{fi})^2 > (V_{fi}^{cr})^2 \equiv \hbar\omega_{\mathrm{eff}}\sqrt{(1/\pi)k_BT\,E_s^{cl}};\quad (V_{fi})^2 > \hbar|v|\Delta F. \tag{3.1}$$

ω_{eff} is the effective frequency of the multi-dimensional potential surfaces,[33] E_r^{cl} is the total classical reorganization free energy, ΔF is the difference in the gradients of the potential surfaces at the crossing, and v is the velocity for motion along the surface in the crossing region.

The relations between the thermal activation energy and the maximum energy for radiative absorption are different in the adiabatic and diabatic limits. We assume here that the exchange coupling is sufficient to ensure full electronic adiabaticity but small enough that a significant barrier on the lower potential surface remains (Fig. 2). Most of the potential surface distortion occurs near the crossing. The activation energy is thus lowered by $2\sqrt{\alpha(1-\alpha)}\,V_{fi}$,[16,17,33] where α is the transfer coefficient of ET theory, i.e.,

$$\alpha = -k_BT\,\mathrm{d}\ln W_{fi}^{\mathrm{th}}/d\Delta G_0. \tag{3.2}$$

If the potential surface distortion near the minima can be disregarded, then the relation between the maxima for optical absorption from the reactants' part of the ground state potential surface and the activation energy for the thermal process is

$$E_A = [(h\nu_m)^2/4(h\nu_m - \Delta G_0)] - 2\sqrt{\alpha(1-\alpha)}\,V_{fi}, \tag{3.3}$$

where α can be obtained in a straightforward manner from Eqs. (2.20)–(2.23) or a similar formalism once the representation of the various system parts is specified.

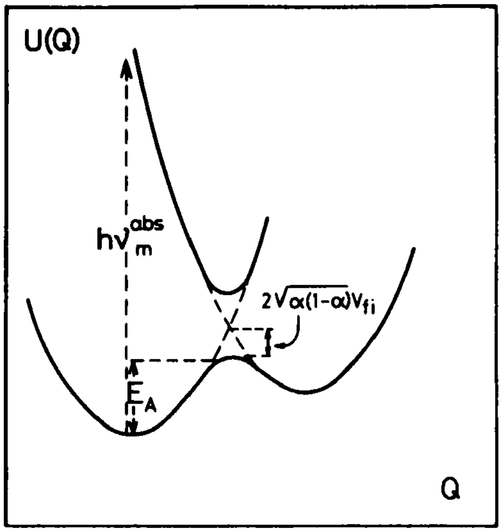

FIGURE 2 Potential surface splitting in the crossing region for adiabatic ET.

4. OPTICAL DETECTABILITY OF THE CROSSING REGION

The electron exchange matrix element, V_{fi}, is at the same time one of the most important and most elusive parameters of ET theory. Direct determination of V_{fi} could in principle be achieved if radiative absorption or emission in the crossing region could be brought to occur. This is, however, excluded in the diabatic limit for which the transition state is a transient, non-stationary configuration. The same applies to absorption in the adiabatic limit, but if the ET system could be prepared in the first excited electronic state of the two adiabatic surfaces, it would then be located in a stationary state with a deep potential well and minimum close to the transition state configuration. The lifetime of this state is determined by the splitting of the surfaces, the fluorescence lifetime, the spectrum of solvent relaxation times, and—for bimolecular transitions—by the intermolecular diffusion time. All these quantities can take suitable values and could lead to long enough lifetimes for observation, as shown by the following points which can be substantiated by the formalism in Section 2:

(A) The splitting in the crossing region determines the rate of non-radiative relaxation. The relaxation probability on multiple passage of the crossing region is, in semiclassical approximation,

$$W_{\mathrm{rel}} = 1 - \left\{1 - e^{-2\pi\gamma} \sum_{n=0}^{\infty} (1 - e^{-2\pi\gamma})^{2n}\right\} = \frac{1}{2 - e^{-2\pi\gamma}} \quad (4.1)$$

where γ is the Landau-Zener parameter

$$\gamma = (V_{fi})^2/\hbar v|\Delta F|. \quad (4.2)$$

In the diabatic limit $W_{\mathrm{rel}} \approx 1 - 2\pi\gamma \approx 1$, i.e., the system rapidly relaxes to the ground state. On the other hand, in the adiabatic limit $W_{\mathrm{rel}} \approx 1/2$. The non-radiative decay channel is here rather inefficient, and unless other decay channels are important, the excited state can remain sufficiently populated for detection.

(B) The excited state may decay radiatively to the ground state. The radiative lifetime is given by Eqs. (2.2) and (2.5) and the formalism in Section 2.2. Radiative decay is unimportant for establishment of vibrational equilibrium in the excited state if τ_r^{-1} is significantly smaller than the effective inverse excited state relaxation time, $(\tau_{\mathrm{rel,eff}}^{\mathrm{ex}})^{-1}$,

$$\tau_r^{-1} << (\tau_{\mathrm{rel,eff}}^{\mathrm{ex}})^{-1} \quad (4.3)$$

in which case the excited state population has still only dropped to 50% by non-radiative relaxation after equilibrium. Even if Eq. (4.3) is not valid, a smaller but still detectable equilibrated excited state population may remain.

(C) A final condition for a significant excited state population relates to intermolecular transitions between mobile molecules. Diffusive motion may lead to a configuration where $2\pi\gamma$ is unfavorable and approaches the diabatic limit of fast non-radiative relaxation. This effect is unimportant if the diffusion time is long compared with the excited state vibrational relaxation time.

A significant excited state population can be prepared by intensive radiation or optical pumping. Provided that vibrational relaxation is fast and the splitting of the potential surfaces in the crossing region large, a substantial part of the population can be expected to survive at equilibrium, the configuration of which corresponds to the transition state. The equilibrium excited state configuration can then be coupled radiatively to the ground state in a twofold fashion both of which in principle can lead to determination of the exchange matrix element. Spontaneous or stimulated light emission leads to emission with a minimum frequency, $\nu_{\mathrm{min}}^{\mathrm{em}}$, at

$$h\nu_{\mathrm{min}}^{\mathrm{em}} = 2V_{fi}. \tag{4.4}$$

This radiation can in principle extend to the far infrared region since adiabaticity already prevails at $V_{fi} \gtrsim k_BT$ ($\approx 200\ \mathrm{cm}^{-1}$ at $T = 298$ K). Alternatively, Raman scattering in the excited state potential well of effective vibrational frequency $\omega_{\mathrm{eff}}^{\mathrm{ex}} = (\tau_{\mathrm{rel,eff}}^{\mathrm{ex}})^{-1}$ may lead to a sequence of anti-Stokes-like scattered line frequencies

$$h\nu = (n + \tfrac{1}{2})\hbar\omega_{\mathrm{eff}}^{\mathrm{ex}} + 2V_{fi} \tag{4.5}$$

corresponding to scattering from a manifold of excited state vibrational levels $\{n\}$ into the electronic ground state (Fig. 3).

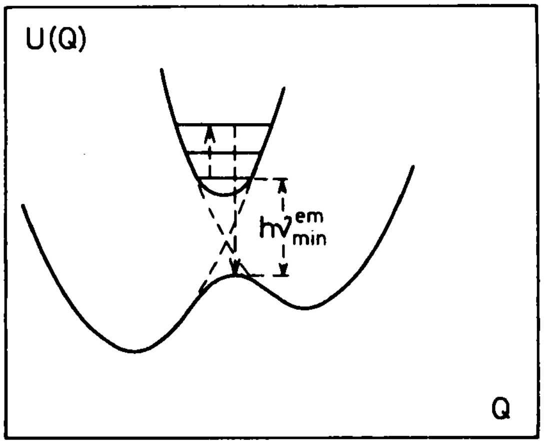

FIGURE 3 Adiabatic potential surfaces which show the minimum frequency for light emission from the excited state and a conceivable electronic–vibrational Raman scattering process.

We conclude by emphasizing that this discussion addresses the principal question of detecting the transition state region by infrared or visible luminescence or by Raman scattering. The conclusion is that such an observation is in principle possible, but no such experiment has yet been carried out.

5. SINGLE-PHOTON TRANSITIONS BETWEEN MOLECULES AND METAL OR SEMICONDUCTOR ELECTRODES

The formalism in Sections 2 and 3 can be extended to interfacial electrochemical ET where electrons are photo-excited from a depolarizer molecule or molecular adsorbate into the continuous electronic spectrum of the metal or semiconductor electrode, or vice versa. The observables here are the cathodic and anodic dark currents, and the photocurrents for a given incoming light intensity in a narrow frequency interval. These observables are quantities integrated over the entire electronic spectrum of the electrode. The cathodic dark current density at given overvoltage, η, is[34]

$$i_c^{\text{dark}}(\eta) = eC\frac{1}{A}\,\delta x\int_{-\infty}^{\infty} d\varepsilon\rho(\varepsilon)n(\varepsilon)\,W_{fi,c}^{\text{dark}}(\varepsilon,\eta) \tag{5.1}$$

where e is the electronic charge, C the depolarizer concentration, A the electrode area, δx the extension of the reaction zone perpendicular to the electrode surface, $\rho(\varepsilon)$ the electrode level density and $n(\varepsilon)$ the Fermi function. $W_{fi,c}^{\text{dark}}$ is finally the probability per unit time for transition from a given level ε to the depolarizer molecule. A similar expression applies to the anodic currents in which $n(\varepsilon)$ is replaced by $1 - n(\varepsilon)$ and $W_{fi,c}^{\text{dark}}$ by the probability for ET from the molecule to the electrode, $W_{fi,a}^{\text{dark}}$.

All electronic levels are suitably referred to the Fermi level ε_F. The cathodic reaction free energy at a given overpotential is then

$$\Delta G_0^c(\varepsilon,\eta) = \Delta G_{0F}^c - (\varepsilon - \varepsilon_F) - e\eta \tag{5.2}$$

with an analogous combination for the anodic process, ΔG_{0F}^c being the reaction free energy for transition at the Fermi energy at equilibrium. $W_{fi,c}^{\mathrm{dark}}(\varepsilon,\eta)$ is then obtained directly from Eqs. (2.1) and (2.9) or (2.20)–(2.24) by insertion of Eq. (5.2).

The cathodic photocurrent is

$$i_c^{\mathrm{ph}}(\eta,\nu) = eC\frac{1}{A}\,\delta x\int_{-\infty}^{\infty} d\varepsilon\rho(\varepsilon)n(\varepsilon)W_{fi,c}^{\mathrm{ph}}(\varepsilon,\eta,\nu) \tag{5.3}$$

where the transition probability for the photoelectrochemical event, $W_{fi,c}^{\mathrm{ph}}(\varepsilon,\eta,\nu)$, is

$$W_{fi,c}^{\mathrm{ph}}(\varepsilon,\eta,\nu) = \frac{4\pi}{3c}\,I_{\mathbf{k}}\,W_{fi,c}^{\mathrm{opt}}\,(\varepsilon,\eta,\nu). \tag{5.4}$$

$I_{\mathbf{k}}$ is the incoming light intensity in a narrow wave number interval around $\mathbf{k}$ and $W_{fi,c}^{\mathrm{opt}}(\varepsilon,\eta,\nu)$ is given by Eq. (2.2) by replacing $\Delta G_0 \pm h\nu$ with $\Delta G_{0F}^{c} - (\varepsilon - \varepsilon_F) - e\eta - h\nu$.

Equations (5.1)–(5.4) also provide the action spectrum for the photo-induced electrochemical process in a form analogous to Eqs. (2.6)–(2.8). If we can disregard the dependence of the electronic factor on ε,[35] then the correlation between the photoelectrochemical and the dark current densities is

$$i_c^{\mathrm{ph}}(\eta,\nu) = \frac{4\pi}{3c}\,I_{\mathbf{k}}[M_{fi}(\mathrm{Q}_{\mathrm{opt}}^{*})/V_{fi}(\mathrm{Q}_{\mathrm{th}}^{*})]^2\; i_c^{\mathrm{dark}}(e\eta - h\nu) \tag{5.5}$$

where $i_c^{\mathrm{dark}}(e\eta - h\nu)$ is obtained from Eq. (5.1) by replacing $e\eta$ by $e\eta - h\nu$.

The following special form of Eq. (5.5) emerges at the equilibrium potential for the dark current:

$$i_c^{\mathrm{ph}}(\eta = 0,\nu) = \frac{4\pi}{3c}\,I_{\mathbf{k}}[M_{fi}(\mathrm{Q}_{\mathrm{opt}}^{*})/V_{fi}(\mathrm{Q}_{\mathrm{th}}^{*})]^2\; i_c^{\mathrm{dark}}(e\eta - h\nu). \tag{5.6}$$

In other words, the effect of photo-excitation is equivalent to an overpotential shift of $e\eta = h\nu$.

Further specification of the correlations between the photocurrent and dark currents at both metal and semiconductor electrodes can straightaway be carried out by combining the formalism in Section 2 with Eqs. (5.1)–(5.6). When the maximum light frequency $h\nu_m \approx E_r + \Delta G_0$, is large, it may, however, approach the plasma frequency for semiconductors which is low for small charge carrier densities. The surface electronic structure and image forces then no longer respond adiabatically to changes in the molecular electronic states, and the transition acquires an altogether different character.

6. LIGHT-INDUCED TRANSITIONS IN THREE-LEVEL SUPEREXCHANGE ET SYSTEMS

The electronic factor in intramolecular ET between donor and acceptor groups separated by "assisting" molecular bridge groups is composed of the molecular orbitals of both donor and acceptor groups and of all the intermediate bridge group orbitals. The resulting overall ET proceeds as a multi-electron transition, in the higher order perturbative limit denoted superexchange[36–40] which clearly dominates over both direct ET and superexchange ET via solvent bridge group molecules. Intervalence light-induced ET in molecules and solid state systems also always involves donor and acceptor groups covalently linked to bridge group molecules. Light-induced transitions can therefore also be expected to possess a higher channel. We conclude our overview of correlations between thermal and optical ET by a short investigation of such correlations for higher order processes. We restrict ourselves to second order processes in which the donor, the acceptor, and a single bridge group level are all strongly coupled to the environments, and for which a comprehensive formalism is now available.[39,41] We also restrict our considerations to classical nuclear motion. Handling of the relaxation of this restriction is available elsewhere.[39,41,42]

We first overview briefly some elements of superexchange ET theory in a three-level system. We then proceed to an analysis of the correlation between the superexchange rate constant and various single-photon absorption processes, and we conclude by briefly addressing Raman scattering processes in such systems.

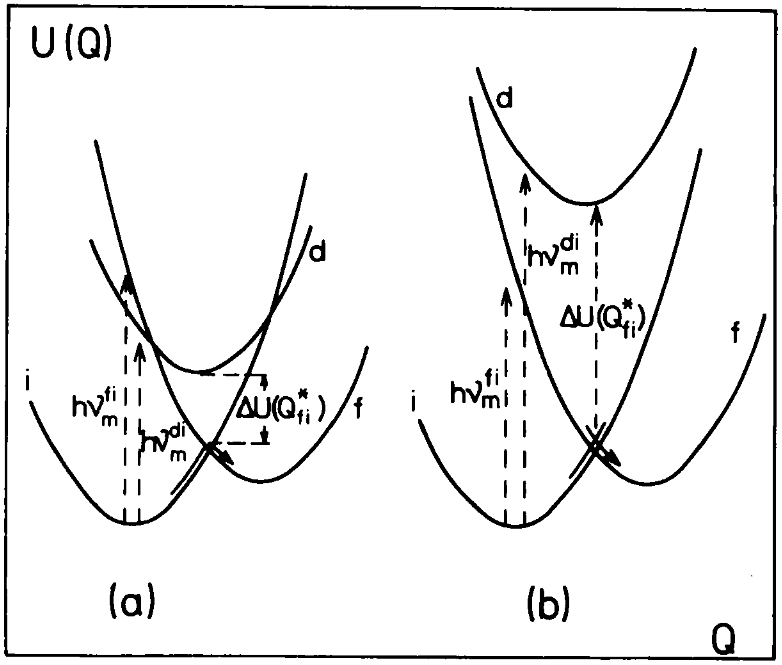

FIGURE 4 Potential surfaces of three-level transitions through high-energy intermediate electronic states. The thermal process is indicated by the fully drawn arrows. The maximum frequencies for the $i \rightarrow d$ and $i \rightarrow f$ transitions are ν_m^{di} and ν_m^{fd}, respectively, and the transitions are indicated by dashed arrows. (a) $\nu_m^{di} < \nu_m^{fd}$; (b) $\nu_m^{di} > \nu_m^{fd}$.

6.1. Thermal Superexchange ET

The thermal superexchange ET rate constant is[39,41,42]

$$W_{fi}^{\mathrm{th}(2)}(\Delta G_0) = \frac{2\pi}{\hbar} Z_i^{-1} \sum_{n_i, n_f} \exp(-\beta E_{n_i}) \left| \sum_{n_d} \frac{\langle i | V_{di}^{(1)} | d \rangle \langle d | V_{fd}^{(1)} | f \rangle}{E_{n_i} - E_{n_d} + i\gamma} \right|^2$$

$$\times\, \delta(E_{n_i} - E_{n_f} - \Delta G_0); \quad \gamma \rightarrow 0; \qquad (6.1)$$

$$Z_i = \exp(\beta G_i) = \sum_{n_i} \exp(-\beta E_{n_i})$$

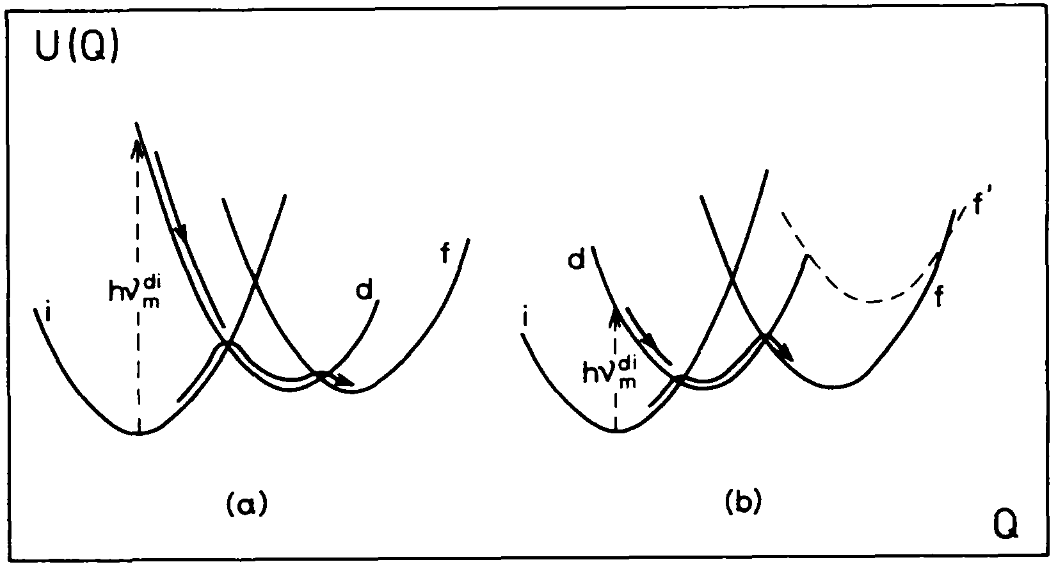

FIGURE 5 Potential energy surfaces for three-level transitions through vibrationally unrelaxed low-energy intermediate states. Optical and thermal processes indicated as in Fig. 4. (a) $U_{di}^* > U_{fd}^*$; (b) $U_{di}^* < U_{fd}^*$. The potential surface f' in Fig. 5(b) is too high for photo-induced $i \rightarrow f'$ ET, cf. text.

where $V_{di}^{(1)}$ and $V_{fd}^{(1)}$ are the first order matrix elements which couple the intermediate state "d" with the initial ("i") and final ("f") states. $|i\rangle$, $|d\rangle$ and $|f\rangle$ represent the complete manifolds of molecular and solvent vibrational wave functions in the three electronic states, while E_{n_i}, E_{n_d}, E_{n_f} and n_i, n_d, n_f are the corresponding sets of vibrational energies and quantum numbers, respectively.

The superexchange rate constant exhibits a more entangled pattern than first order transitions due to the manifold of vibrational levels in the denominators of Eq. (6.1). Quasiclassical,[39a] trajectory,[39d] and quantum mechanical calculations[39c] show that two major patterns emerge depending on whether the intermediate state energy is "high" or "low" in the sense of Figs. 4 and 5. We consider in turn these two limits. For the sake of simplicity we restrict ourselves to diabatic transitions in three one-dimensional displaced harmonic oscillators of frequency ω, but generalization to multidimensional surfaces and to adiabatic processes can be achieved by procedures reported elsewhere.[39d,41]

6.1.1. *Superexchange ET via "High-Energy" Intermediate States*

In this limit (Fig. 4) $W_{fi}^{\mathrm{th}(2)}(\Delta G_0)$ coincides with that for direct ET at the crossing between the initial and final state surfaces except that the electronic factor is of second order and involves coupling to the high-energy intermediate state. The energy denominator depends weakly on the coordinate Q and can be replaced by its value at the crossing, Q_{fi}^*. Using also the closure relation for the intermediate states, $\Sigma_{n_d}|d\rangle\langle d| = 1$, we obtain, from Eq. (6.1),

$$W_{fi}^{\mathrm{th}(2)}(\Delta G_0) = \frac{2\pi}{\hbar} Z_i^{-1} \left(\frac{V_{di}^{(1)} V_{fd}^{(1)}}{\Delta U(\mathbf{Q}_{fi}^*)} \right)^2$$

$$\times \sum_{n_i, n_f} \exp(-\beta E_{n_i}) |\langle i|f\rangle|^2 \, \delta(E_{n_i} - E_{n_f} - \Delta G_0). \quad (6.2)$$

Apart from the electronic factor this form coincides with the rate constant for first order transitions at the point Q_{fi}^*, and we obtain

$$W_{fi}^{\mathrm{th}(2)}(\Delta G_0^{fi}) = \left(\frac{\pi}{\hbar^2 k_B T E_r^{fi}} \right)^{1/2} \left(\frac{V_{di}^{(1)} V_{fd}^{(1)}}{\Delta U(Q_{fi}^*)} \right)^2 \exp\left[-\frac{(E_r^{fi} + \Delta G_0^{fi})^2}{4 E_r^{fi} k_B T} \right] \quad (6.3)$$

where superscripts have been added to ΔG_0 and the reorganization energy to characterize the particular transitions.

6.1.2. *Superexchange ET via "Low-Energy" Intermediate States*

In this limit the activation energy is determined by the crossing point of highest energy involving the intermediate state. The rate constant, derived elsewhere,[39] is

$$W_{fi}^{\text{th}(2)}(\Delta G_0^{fi}) = \left(\frac{\pi^3}{k_B T E_r^{di} E_r^{fd} |U_{di}^* - U_{fd}^*|}\right)^{1/2} \times \frac{(V_{di}^{(1)} V_{fd}^{(1)})^2}{\hbar^2 \omega} \exp[-\beta(U^* - U_{i0})] \tag{6.4}$$

where U^* is the highest crossing point energy involving the intermediate state, i.e.,

$$\begin{aligned} U^* &= U_{fi}^* = \frac{1}{4E_r^{di}}(E_r^{di} + \Delta G_0^{di})^2 \quad \text{if } U_{di}^* > U_{fd}^*, \\ U^* &= U_{fd}^* = \Delta G_0^{di} + \frac{1}{4E_r^{fd}}(E_r^{fd} + \Delta G_0^{fd})^2 \quad \text{if } U_{di}^* < U_{fd}^*. \end{aligned} \tag{6.5}$$

Equation (6.4) can be written in a form which contains two Landau–Zener factors, say for $U_{di}^* > U_{fd}^*$:

$$W_{fi}^{\text{th}(2)}(\Delta G_0^{fi}) = 4\pi^{3/2}\gamma_{di}\gamma_{fd} \cdot \omega \exp[-\beta(U_{di}^* - U_{i0})] \tag{6.6}$$

where

$$\begin{aligned} \gamma_{di} &= (V_{di}^{(1)})^2/\hbar \cdot v_{di}|\Delta F_{di}|; \\ \gamma_{fd} &= (V_{fd}^{(1)})^2/\hbar \cdot v_{fd}|\Delta F_{fd}|. \end{aligned} \tag{6.7}$$

The velocity at the point of highest energy, v_{di}, corresponds to thermal velocity, the transition at the lower point to a higher velocity where the difference between the potential energies at the two points has been converted to kinetic energy, i.e.,

$$v_{di} = \sqrt{2\frac{\omega}{\hbar}k_B T}; \quad v_{fd} = \sqrt{2\frac{\omega}{\hbar}|U_{di}^* - U_{fd}^*|}. \qquad (6.8)$$

This form is notable, and together with the appearance of *two* electronic coupling factors in Eqs. (6.4) and (6.7) it emphasizes the vibrationally unrelaxed nature of the intermediate state and the character of the overall process as a single elementary act.

We now take Eqs. (6.2)–(6.8) as a basis for correlations between thermal superexchange ET and optical single- and two-photon processes in electronic three-level systems.

6.2. Single-Photon Absorption in Electronic Three-Level Systems and Relations to Thermal Superexchange ET

We consider optical single-photon absorption separately for systems with high- and low-energy intermediate states. It is assumed that the overall photo-induced transition from the initial to the final state can occur either by absorption resonances directly between the "i" and "f" states or by $i \rightarrow d$ resonances.

6.2.1. *High-Energy Intermediate States*

The levels may be located in the two ways shown in Figs. 4(a) and 4(b) where the latter is representative of the large group of well characterized mixed-valence ruthenium complexes. The $i \rightarrow f$ transition may also be induced by two-photon processes where Fig. 4(a) would correspond to two-photon absorption and Fig. 4(b) to Raman scattering. We finally assume that the system is initially equilibrated in the state "i" so that absorption only from this state needs to be considered. The following cases can then be distinguished:

6.2.1.1. *Direct transition between the initial and final states.* This case is fully covered by the formalism in Section 2 and is normally what is considered for intervalence transitions in binuclear transition metal complexes. The energies of the metal-to-bridge group transitions in these systems are high and correspond to Fig. 4(b).

6.2.1.2. *Indirect transition via resonance between initial and intermediate states.* The $i \rightarrow f$ transition may also be induced by $i \rightarrow d$ resonance absorption corresponding for example to the strongly allowed donor/bridge group charge transfer bands in mixed-valence complexes. This is followed by nonradiative electronic relaxation of the intermediate state. Such a path corresponds to the second ET mechanism described in Section 6.1.2. The molar absorptivity is (cf. Eqs. (2.2) and (6.1))

$$\kappa_{fi}^{(2)}(\nu) = \frac{2\pi}{3c} h\nu W_{fi}^{\mathrm{opt}(2)}(\nu), \tag{6.9}$$

$$W_{fi}^{\mathrm{opt}(2)}(\nu) = \frac{2\pi}{\hbar} Z_i^{-1} \sum_{n_i, n_f} e^{-\beta E_{n_i}} \left| \sum_{n_d} \frac{\langle i | M_{di}^{(1)} | d \rangle \langle d | V_{fd}^{(1)} | f \rangle}{E_{n_i} - E_{n_d} + h\nu + i\gamma} \right|^2$$

$$\times \delta(E_{n_i} - E_{n_f} - \Delta G_0^{fi} + h\nu) \tag{6.10}$$

in other words, the states $|i\rangle$ and $|d\rangle$ are coupled radiatively, $|d\rangle$ and $|f\rangle$ nonradiatively. With reference to Fig. 4 and Sections 6.1.1 and 6.1.2, Eqs. (6.9) and (6.10) can straightaway be recast into forms identical to Eqs. (6.4)–(6.8) except that $V_{di}^{(1)}$ is now everywhere replaced by $M_{di}^{(1)}$, ΔG_0^{di} by $\Delta G_0^{di} - h\nu$, and ΔG_0^{fi} by $\Delta G_0^{fi} - h\nu$. Specifically (cf. Eq. (2.6))

$$\kappa_{fi}^{(2)}(\nu) = \frac{2\pi}{3c} h\nu \left[M_{di}^{(1)}(Q_{\mathrm{opt}}^*)/V_{di}^{(1)}(Q_{th}^*)\right]^2 W_{fi}^{\mathrm{th}(2)}(\Delta G_0^{fi} - h\nu). \tag{6.11}$$

6.2.1.3. *Indirect transition via resonance between initial and final states.* Due to the poor direct overlap between the donor and acceptor states, the $i \rightarrow f$ resonance transition may proceed more favorably by off-resonance coupling to a high-energy intermediate state, i.e., "virtually." This case corresponds to Fig. 4(b) and the off-resonance case in Section 6.1.1. The electronic factor has the same form as in Eq. (6.10) where the energy denominator can also be written as

$$E_{n_i} - E_{n_d} - \Delta G_0^{di} + h\nu \approx h\nu_m^{di} - h\nu_m^{fi}. \tag{6.12}$$

The correlation between the optical and thermal superexchange parameters is again given by Eq. (6.9) where

$$W_{fi}^{\mathrm{opt}(2)}(\nu) = \left(\frac{M_{di}^{(1)}}{V_{di}^{(1)}} \frac{\Delta U(Q_{fi}^{*})}{h\nu_m^{di} - h\nu_m^{fi}}\right)^2 W_{fi}^{\mathrm{th}(2)}(\Delta G_0^{fi} - h\nu). \quad (6.13)$$

It is of interest to compare the molar absorptivities for the direct and off-resonance superexchange light-induced processes. By Eqs. (2.4), (6.3), (6.9) and (6.13) we obtain

$$\kappa_{fi}^{(2)}(\nu)/\kappa_{fi}^{(1)}(\nu) = \left(\frac{1}{h\nu_m^{di} - h\nu_m^{fi}} \frac{M_{di}^{(1)}(Q_{\mathrm{opt}}^{*})\, V_{fd}^{(1)}(Q_{\mathrm{opt}}^{*})}{M_{fi}^{(1)}(Q_{\mathrm{opt}}^{*})}\right)^2. \quad (6.14)$$

$h\nu_m^{di} - h\nu_m^{fi}$ is not likely to exceed $V_{fd}^{(1)}$ by more than an order of magnitude. Since $M_{di}^{(1)} >> M_{fi}^{(1)}$ the ratio in Eq. (6.14) can therefore be significant and the superexchange transition expected to be fully competitive or dominate.

6.2.2. *Low-Energy Intermediate States*

In contrast to the cases in Section 6.2.1, the $i \rightarrow d$ transition is now always at much lower energies than the $i \rightarrow f$ transition, and we only need to consider optical resonance with the intermediate state. When $U_{di}^{*} > U_{fd}^{*}$ we obtain straightaway, by the procedures in Section 6.2.1,

$$\kappa_{fi}^{(2)}(\nu) = \frac{2\pi}{3c} h\nu[M_{di}^{(1)}(Q_{\mathrm{opt}}^{*})/V_{di}^{(1)}(Q_{\mathrm{th}}^{*})]^2\, W_{fi}^{\mathrm{th}(2)}(\Delta G_0^{di} - h\nu) \quad (6.15)$$

(cf. Eqs. (2.4) and (6.9)). For this potential surface location Eq. (6.15) applies also when the $d \rightarrow f$ transition belongs to the adiabatic limit.

In the opposite case when $U_{di}^{*} < U_{fd}^{*}$, efficient ET only occurs when light absorption brings the new location of U_{fd}^{*} to a value below the new U_{di}^{*}, in which case Eq. (6.15) remains valid. If U_{fd} is too high for the two crossing points to be inverted on light absorption then the photo-excited electron returns to the initial ground state rather than proceeding to the acceptor state (cf. the surface f' in Fig. 5(b)).

We note in conclusion that the ET path represented by Eq. (6.15) constitutes a most efficient mechanism for charge separation over large distances. In relation to the primary events of bacterial photosynthesis[43–45] and very recent data pointing to population of an electronic state on auxiliary bacteriochlorophyll monomer,[46] the mechanism could be a suitable representation of the overall primary ET from photo-excited bacteriochlorophyll dimer to pheophytin. The initial, intermediate and final states then correspond to "excess" electron localization on bacteriochlorophyll dimer, on the monomer, and on pheophytin, respectively.

7. CORRELATIONS INVOLVING RAMAN SCATTERING CROSS SECTIONS AND SUPEREXCHANGE ET RATE CONSTANTS

It can be expected that suitable locations of the potential surfaces in a three-level ET system can also serve as a basis for correlations between the superexchange ET rate constant and differential cross sections for Raman and resonance Raman scattering. Such correlations have indeed been investigated recently in considerable detail.[41] We conclude our discussion of correlations between optical and thermal processes by an example of such correlations involving off-resonance Raman scattering.

The observable in Raman scattering of a narrow beam of incoming photons centered at the frequency ν into the solid angle element $\Delta\Omega$ and frequency range $\Delta\nu'$ centered at ν' is the differential scattering cross section

$$\frac{\Delta^2\sigma}{\Delta\nu'\Delta\Omega} = \frac{1}{6\pi^2} c^{-4} h^2 \nu (\nu')^3 \, W_{fi}^{\mathrm{scat}}(\nu,\nu'). \tag{7.1}$$

The transition probability, given by second order perturbation theory,

$$W_{fi}^{\mathrm{scat}}(\nu,\nu') = \frac{2\pi}{\hbar} Z_i^{-1} \sum_{n_i,n_f} e^{-\beta E_{ni}} \left| \sum_{n_d} \frac{\langle i|M_{di}^{(1)}|d\rangle\langle d|M_{fd}^{(1)}|f\rangle}{E_{n_i} - E_{n_d} - \Delta G_0^{di} + h\nu} \right|^2$$

$$\times\, \delta(E_{n_i} - E_{n_f} - \Delta G_0^{fi} + h\nu - h\nu') \tag{7.2}$$

reveals that conceptual and formal relations to superexchange ET rate constants must exist. The appearance of the incoming light frequency in both the energy denominator and the delta function of Eq. (7.2) means, however, that the correlations are only simply derived for off-resonance scattering where the energy denominator depends weakly on ν and the vibrational excitation in the three electronic states. As $h\nu$ approaches resonance between the initial and intermediate states, the summation with respect to all the n_d-states in Eq. (7.2) requires a special analysis, details of which are given elsewhere.[41]

The following simple relation between the differential Raman scattering cross section and the superexchange ET rate constant is valid for off-resonance Raman scattering in representative three-level systems of "high" intermediate state energy (Fig. 4):

$$\frac{\Delta^2\sigma}{\Delta\nu'\Delta\Omega} \approx \frac{1}{6\pi^2} c^{-4} h^2 \nu (\nu')^3 \left(\frac{M_{di}^{(1)}(Q_{\text{opt}}^*) M_{fd}^{(1)}(Q_{\text{opt}}^*)}{V_{di}^{(1)}(Q_{\text{th}}^*) V_{fd}^{(1)}(Q_{\text{th}}^*)} \frac{\Delta U(Q_{\text{th}}^*)}{h\nu_m^{di} - h\nu} \right)^2 W_{fi}^{\text{th}(2)}(\Delta G_0^{fi} + h\nu' - h\nu). \qquad (7.3)$$

This equation and a range of other correlations for resonance and off-resonance Raman scattering in electronic three-level systems strongly coupled to the nuclear motion[41] opens exciting new possibilities of combining superexchange ET theory with the theory of Raman scattering in solute molecular systems.

8. CONCLUDING REMARKS

We have overviewed several correlations between the kinetic parameters of thermal and optical two-site ET reactions. The correlations rest on the observables of the various processes, such as the molar absorptivity for light absorption, and the spectral distribution or radiative lifetime for spontaneous emission, rather than solely on the transition probabilities. Two main outcomes emerge from the discussion. The first is that the transition state nuclear configuration and the electron exchange integral in this region are in principle observable by optical emission or Raman scattering from the first excited electronic state, but only in the adiabatic limit. Secondly, we have extended the correlations to superexchange ET rate constants in electronic three-level systems. These correlations link the superexchange rate constants to the molar absorptivity of single-photon processes involving the same three levels. The variety of ET mechanisms that the correlations represent could have some wider implications relating to optical bandshape analysis, to photo-induced reactions in vibrationally unrelaxed multi-level systems, and to long-range charge separation such as in photobiological processes.

Acknowledgments

We would like to thank the Danish National Science Research Council, Fisker og Nielsens Fond, and Otto Mønsteds Fond for financial support.

References

1. S. I. Pekar, *Untersuchungen über die Elektronentheorie der Kristalle* (Akademie Verlag, Berlin, 1954).
2. R. Kubo and Y. Toyozawa, Progr. Theor. Phys. **13**, 160 (1955).
3. N. S. Hush, Progr. Inorg. Chem. **8**, 391 (1967).
4. N. S. Hush, Electrochim. Acta **13**, 1005 (1968).
5. M. B. Robin and P. Day, Adv. Inorg. Chem. Radiochem. **10**, 247 (1967).
6. For a review, see C. Creutz, Progr. Inorg. Chem. **30**, 1 (1983).
7. R. A. Marcus and N. Sutin, Comments Inorg. Chem. **5**, 119 (1986).
8. H. E. Toma and J. M. Malin, J. Am. Chem. Soc. **97**, 288 (1975).
9. A. J. Mirailles, R. E. Armstrong and A. Haim, J. Am. Chem. Soc. **99**, 1416 (1977).
10. R. W. Callahan, F. R. Keene, T. J. Meyer and D. J. Salmon, J. Am. Chem. Soc. **99**, 1064 (1977).
11. G. M. Brown, H. J. Krentzien, M. Abe and H. Taube, Inorg. Chem. **18**, 3374 (1979).
12. C. Creutz, P. Kroger, T. Matsubara, T. L. Netzel and N. Sutin, J. Am. Chem. Soc. **101**, 5442 (1979).
13. T. A. Marsagishvili and D. E. Khoshtariya, Khim. Fiz. **6**, 1511 (1987).
14. I. B. Bersuker, Nouv. J. Chim. **4**, 139 (1980).
15. L. D. Landau and E. M. Lifshitz, *Quantum Mechanics* (Pergamon, Oxford, 1965).
16. R. R. Dogonadze and A. M. Kuznetsov, *Physical Chemistry. Kinetics* (VINITI, Moscow, 1973).
17. R. R. Dogonadze and A. M. Kuznetsov, Progr. Surf. Sci. **6**, 1 (1975).
18. A. M. Kuznetsov, J. Ulstrup and M. A. Vorotyntsev, *The Chemical Physics of Solvation. Part C. Solvation in Specific Physical, Chemical and Biological*

Systems, eds. R. R. Dogonadze, E. Kálmán, A. A. Kornyshev and J. Ulstrup (Elsevier, Amsterdam, 1988), p. 163.

19. R. R. Dogonadze, E. M. Itskovitch, A. M. Kuznnetsov and M. A. Vorotyntsev, J. Phys. Chem. **79**, 2827 (1975).
20. E. M. Itskovitch, J. Ulstrup and M. A. Vorotyntsev, *The Chemical Physics of Solvation. Part B. Spectroscopy of Solvation*, eds. R. R. Dogonadze, E. Kálmán, A. A. Kornyshev and J. Ulstrup (Elsevier, Amsterdam, 1986), p. 223.
21. A. M. Kuznetsov, Nouv. J. Chim. **5**, 427 (1981).
22. A. M. Kuznetsov and J. Ulstrup, Faraday Discussions Chem. Soc. **74**, 31 (1982).
23. A. M. Kuznetsov and J. Ulstrup, *Tunnelling*, eds. J. Jortner and B. Pullman (Reidel, Dordrecht, 1986), p. 345.
24. A. A. Ovchinnikov and M. Ya. Ovchinnikova, Zhur. Eksp. Teor. Fiz. **56**, 1278 (1969).
25. R. R. Dogonadze, A. M. Kuznetsov, M. G. Zakaraya and M. A. Vorotyntsev, J. Electroanal. Chem. **75**, 315 (1977).
26. E. M. Itskovitch and A. M. Kuznetsov, Elektrokhimiya **16**, 755 (1980).
27. D. N. Zubarev, *Non-equilibrium Statistical Thermodynamics* (Plenum, New York, 1974).
28. H. A. Fröhlich, *Theory of Dielectrics* (Clarendon, Oxford, 1958).
29. J. Ulstrup and J Jortner, J. Chem. Phys. **63**, 4358 (1975).
30. J. Ulstrup, *Charge Transfer Processes in Condensed Media* (Springer-Verlag, Berlin, 1979).
31. R. A. Marcus, Disc. Faraday Soc. **29**, 21 (1960).
32. R. A. Marcus and N. Sutin, Biochim. Biophys. Acta **811**, 265 (1985).
33. R. R. Dogonadze and Z. D. Urushadze, J. Electroanal. Chem. **32**, 235 (1971).
34. R. R. Dogonadze, *Reactions of Molecules at Electrodes*, ed. N. S. Hush (Wiley, New York, 1971), p. 135.
35. A. M. Kuznetsov, J. Electroanal. Chem. **151**, 227 (1983).
36. P. W. Anderson, Phys. Rev. **79**, 350 (1950).
37. J. Halpern and L. E. Orgel, Disc. Faraday Soc. **29**, 32 (1960).
38. H. M. McConnell, J. Chem. Phys. **35**, 508 (1961).
39. (a) M. V. Vol'kenshtein, R. R. Dogonadze, A. K. Madumarov and Yu. I. Kharkats, Dokl. Akad. Nauk SSSR, Ser. Fiz. Khim. **199**, 124 (1971). (b) R. R. Dogonadze, J. Ulstrup and Yu. I. Kharkats, J. Electroanal. Chem. **39**, 47 (1972). (c) Yu. I. Kharkats, A. K. Madumarov and M. A. Vorotyntsev, J. Chem. Soc. Faraday Trans. II **70**, 1578 (1974). (d) A. M. Kuznetsov and Yu. I. Kharkats, Elektrokhimiya **12**, 1277 (1976).
40. M. Bixon and J. Jortner, *Protein Structure. Molecular and Electronic Reactivity*, eds. R. Austin, E. Bukhs, B. Chance, D. DeVault, H. Frauenfelder and V. I. Gol'danskij (Springer-Verlag, New York, 1987), p. 277.
41. M. G. Zakaraya and J. Ulstrup, Chem. Phys. **135**, 49 (1989).
42. A. M. Kuznetsov and J. Ulstrup, J. Chem. Soc. Faraday Trans. II **78**, 1398 (1982).
43. *Antennas and Reaction Centres of Photosynthetic Bacteria*, ed. M. E. Michel-Beyerle (Springer-Verlag, Berlin, 1985).
44. *The Photosynthetic Bacterial Reaction Center. Structure and Dynamics*, eds. J. Breton and A. Verméglio (Plenum, New York, 1988).
45. *Perspectives in Photosynthesis*, eds. J. Jortner and B. Pullman (Kluwer, Dordrecht, 1990).
46. W. Holzapfel, U. Finkele, W. Kaiser, D. Oesterhelt, H. Scheer, H. U. Stilz and W. Zinth, Chem. Phys. Lett. **160**, 1 (1989).